

# Targeting and Control of Synchronization in Chaotic Oscillators

E. Padmanaban, Ranjib Banerjee, Ioan Grosu and Syamal K. Dana, *IEEE Member*

**Abstract-** A method of targeting synchronization and its control is reported in chaotic oscillators. This proposes design of appropriate coupling using an open-plus-closed-loop (OPCL) scheme based on Hurwitz stability to establish a desired state of synchrony between the oscillators. In the synchronization state, a chaotic attractor can be scaled up or down in size relative to another attractor. Additionally, a technique of controlling synchronization is introduced that allows a smooth transition from complete synchronization to antisynchronization or vice versa, by tuning a system parameter without loss of stability. A smooth scaling of the size of the attractor is also implemented. The general theory of the coupling definition is described for unidirectional as well as bi-directional mode. Numerical examples are given using a Sprott system. Physical realization of the OPCL coupling and control of synchronization is demonstrated in electronic circuit.

**Index-**Synchronization, chaotic oscillator, coupling design, Sprott circuit.

## I. INTRODUCTION

Chaotic trajectories under coupling converge in the long run to establish a state of synchrony: weak or strong correlation [1-4]. This knowledge encouraged studies on its applicability in secure digital communication. In the last three decades, some successes were certainly achieved such as chaos communication via public domain fiber-optic links [5]. However, the main limitation [6-9] of the existing techniques lies in instabilities due to parameter mismatch and presence of noise. To circumvent the problems, rigorous investigations were done to understand the onset of synchronization and their stability. In the process, a variety of possible coherent states were observed in chaotic oscillators: complete synchronization (CS) or antisynchronization (AS), lag synchronization (LS), phase synchronization (PS), antiphase synchronization (APS), generalized synchronization (GS). In case of CS [3], two chaotic trajectories become identical in amplitude and phase in time. In case of AS, two trajectories are identical in amplitude but opposite in phase. Two chaotic trajectories are identical in amplitude but maintain a constant lag in case of LS [10-11]. Chaotic trajectories maintain a constant phase difference but their amplitudes remain uncorrelated in PS [12-13]. APS [13-14] is opposite to PS: no correlation in amplitude but maintain opposite phase in time. In case of GS [15], two trajectories have no apparent correlation but maintain a functional relationship.

Various coupling configurations, unidirectional, mutual or bidirectional coupling were tried and also special types of coupling such as inhibitory [16] or excitatory [17] and repulsive [18] were investigated, particularly, in context of neuron dynamics.

This work is partially supported by the BRNS/DAE, India under grant BRNS/34/26/2009. E. Padmanaban (padmanaban@iicb.res.in), Ranjib Banerjee (ranjib\_b@gmail.com), Syamal K. Dana (skdana@iicb.res.in) are with the Indian Institute of Chemical Biology, Jadavpur, Kolkata 700032, India and Ioan Grosu was with the Faculty of Bioengineering, University of Medicine and Pharmacy, "Gr. T. Popa," Iasi, Romania.

Major efforts of the investigations was concentrated on playing with the coupling strength and the mismatch parameters or noise strength to observe the onset of different synchronization regimes and their instabilities in two or more oscillators. Under such linear diffusive coupling, all different synchronization regimes, CS or AS, LS and PS, APS were observed by varying the coupling strength but above different critical coupling intercepted [13-14] by intermediate desynchronization regimes.

On the other hand, engineering synchronization [19-21] in nonlinear oscillators is recently given importance for practical purposes. It assumes the definition of a dynamical system as known, then addresses a question how to define an appropriate coupling to realize a desired state of synchronization in an assembly of the given systems and also to ensure stability. It is reported [22-24] by the authors that, once the definition of a model system is known, one can always define a coupling to establish a desired synchronization state between chaotic oscillators, either CS, AS or amplitude death (AD) using an OPCL scheme based on Hurwitz stability [24]. A driver attractor can also be scaled up or down (amplified or attenuated) in size at the response exactly at a pre-defined value. This coupling differs from the usual simple linear diffusive form, yet it is not difficult to implement physically. In engineering applications, an additional requirement is accessibility of tunable parameters necessary for a precise and smooth control of synchronization.

In this paper, the issue of engineering synchronization in chaotic oscillators is further explored using the OPCL coupling. The method was so far unable to realize AS in any system under bidirectional mode excepting inversion symmetric systems. The theory is extended here to remove this restriction. Next, a method of controlling synchronization is introduced, particularly, for unidirectional mode. Given a model system and a target synchronization state, the coupling is defined analytically to establish the desired of synchronization state between two oscillators and then physically implemented that incorporates a smooth control from one to the other form of synchronization, namely, from CS to AS or *vice versa* using a tunable system parameter. The attractor size is also allowed to be varied continuously and smoothly. By smooth control, it is meant that no loss of stability in synchronization occurs during the transition from CS to AS or *vice versa*. This is in contrast to what is usually observed for linear diffusive coupling. The present study uses a Sprott system for numerical examples. Experimental realization of the coupling and control of synchronization is also demonstrated using electronic circuits of the Sprott system.

The paper is organized as follows: theory of OPCL coupling is explained in section II. In section IIIA, the bidirectional coupling is elaborated for CS and AS using numerical examples of a Sprott system. In section IV, experimental verifications of unidirectional and bi-directional OPCL schemes are described. Results are summarized in section V.

## II. OPEN-PLUS-CLOSED-LOOP COUPLING: THEORY

The OPCL coupling was investigated [22-24] earlier to realize CS and AS with amplification (or attenuation) in chaotic oscillators using unidirectional coupling. A physical realization of the coupling was also demonstrated in electronic circuit. The theory was later extended [24] to bidirectional coupling but it was found restricted to inversion symmetric system only in the AS mode. The theory is extended here to rule out the restriction and to generalize it for any chaotic system. Two chaotic oscillators are defined by

$$\dot{x} = f(x) \text{ and } \dot{y} = f(y) \quad x, y \in R^n \quad (1)$$

If the oscillators are mutually coupled to achieve a goal dynamics,

$$g_1 = \alpha x \text{ or } g_2 = \frac{y}{\alpha}, \quad (2)$$

the coupled chaotic system is defined by

$$\dot{x} = f(x) + D_x(x, g_2), \quad (3a)$$

$$\dot{y} = f(y) + D_y(y, g_1), \quad (3b)$$

where  $\alpha$  is a constant. A general definition of the coupling functions is given,

$$D_x(x, g_2) = S_x(H - J_1 f(y))(x - g_2), \quad (3c)$$

$$D_y(y, g_1) = S_y(H - J_2 f(g_1))(y - g_1) + \alpha f(x) - f(g_1) \quad (3d)$$

where  $J_1=(\partial/\partial y)$  and  $J_2=(\partial/\partial g_1)$  are the *Jacobian* of the interacting dynamical systems.  $H$  is an arbitrary  $n \times n$  constant matrix and  $S_x, S_y$  are the constants which act as switches to configure either unidirectional or bidirectional coupling. For mutual or bidirectional coupling,  $S_x=S_y=0.5$  and for master-slave or unidirectional coupling,  $S_x=0, S_y=1$ . The error function of the coupled system is,

$$e = (y - \alpha x) \text{ or } e = (y - g_1) \quad (4)$$

and the error dynamics is

$$\dot{e} = (\dot{y} - \alpha \dot{x}) \quad (5)$$

when  $f(y)$  can be written, using Taylor's series expansion, as

$$f(y) = f(g_1 + e) = f(g_1) + \frac{\partial f(g_1)}{\partial (g_1)} e + \dots \quad (6)$$

Using an approximation of a small error  $e$ , the Taylor's expansion is truncated upto the first order derivative in (6) and substituted in (3b). Assuming a state of stable synchronization when  $e \rightarrow 0$  for  $t \rightarrow \infty$  and substituting  $y = \alpha x$  or  $y = g_1$  in (3c), the

error dynamics is obtained as  $\dot{e} = He$  from (5). This indicates that the error dynamics has a zero steady state ( $e \rightarrow 0, t \rightarrow \infty$ ) if the  $H$  matrix has eigenvalues all with negative real parts, *i.e.*  $H$  matrix becomes a Hurwitz. A state of asymptotically stable synchronization is established.

The essential factor in defining the coupling in 3(c)-(d) is the appropriate selection of the elements of the  $H$  matrix to realize a stable synchronization state. All other parameters are known from the definition of the dynamical system except the constant  $\alpha$  which can be chosen arbitrarily and varied continuously. The  $H$  matrix is constructed from the *Jacobian* of the model flow of the interacting oscillators: the elements of the matrix,  $H_{ij}$ , are chosen same as  $H_{ij}=(\partial f(g_1)/\partial g_1)_{ij}$  when  $(\partial f(g_1)/\partial g_1)_{ij}$  is a constant in a *Jacobian*. If  $(\partial f(g_1)/\partial g_1)_{ij}$  involves any state variable, it is replaced by a constant  $p_i$ . Once the  $H$  matrix is defined it has to satisfy a Routh-Hurwitz (RH) criterion [23-24] to confirm that eigenvalues of  $H$  matrix all have negative real parts. For a 3D system, as example, the  $H$  matrix ( $3 \times 3$ ) has a characteristic equation,

$$\lambda^3 + a_1 \lambda^2 + a_2 \lambda + a_3 = 0 \quad (7a)$$

where  $a_i (i=1,2,3)$  is a constant and the RH criterion is given by

$$a_1 > 0, \quad a_1 a_2 - a_3 > 0, \quad a_3 > 0. \quad (7b)$$

The  $a_i$  parameters of (7a) can be expressed in terms of the  $p_i$  parameters of the  $H$  matrix to realize the RH criterion. The stability of synchronization is thus ensured by an appropriate choice of  $p_i$ . Then the sign of  $\alpha$  decides whether it is CS or AS and its magnitude decides the scale of the attractor size (relative amplification or attenuation of attractors). From (3) it is clear that the mutual coupling is symmetric for  $\alpha=1$ , but one can only achieve CS but no amplification or attenuation. The coupling is asymmetric for  $\alpha \neq 1$ , when one can realize both CS and AS and relative scaling (amplification or attenuation) of attractor size. Two different cases arise for asymmetric mutual coupling: the coupling is so designed as to establish stable synchronization by keeping one oscillator size unchanged and to change the size of the other oscillator by varying  $\alpha$ . **Case I:** To maintain synchronization and to change the size of the second oscillator (3b), the goal is set by (2) and the coupling terms are defined by (3c)-(3d) when the error function of the coupled system is defined by (4). **Case II:** To allow changes in the size of the first oscillator (3a) under a state of synchrony, one has to redefine the goal dynamics,

$$g_1 = \frac{x}{\alpha} \text{ or } g_2 = \alpha y$$

when the coupling terms are defined by

$$D_x(x, g_2) = S_x(H - J_1 f(g_2))(x - g_2) + \alpha f(y) - f(g_2) \quad (8a)$$

$$D_y(y, g_1) = S_y(H - J_2 f(x))(y - g_1) \quad (8b)$$

where  $J_1=(\partial/\partial g_1)$  and  $J_2=(\partial/\partial x)$  are the *Jacobian* of the interacting dynamical systems. The error function of the coupled system is also redefined by  $e = (x - \alpha y)$ .

On the other hand, the master slave coupling is always asymmetric and if  $\alpha$  is varied from -1 to 1, a transition from AS to CS or vice versa can be observed with attenuation for intermediate values of  $\alpha$ . Scaling up of attractors (amplification) with a transition from AS to CS or vice versa is possible for a choice of  $|\alpha| > 1$ . The  $\alpha$  parameter is physically made accessible and tuned for smooth control of synchronization. This does not affect the stability of synchronization since the stability depends only upon the Hurwitz parameter  $p_i$ . The control of synchronization is demonstrated experimentally using an electronic version of a Sprott system.

### III. OPCL COUPLING: SPROTT SYSTEM

A Sprott system [25] with a single quadratic nonlinearity is chosen for analysis. This example evidences how OPCL coupling is applicable to any system without restricting to inversion symmetric system in the AS regime. An inversion symmetric system has a dynamical flow that follows a rule,  $f(x) = -f(-x), x \in R^n; f: R^n \rightarrow R^n$ .

Sprott oscillator-1 after coupling:

$$\begin{pmatrix} \dot{x}_1 \\ \dot{x}_2 \\ \dot{x}_3 \end{pmatrix} = \begin{pmatrix} -b_1 \cdot x_2 \\ x_1 + x_3 \\ x_1 + x_2^2 - x_3 \end{pmatrix} + \begin{pmatrix} D_{x_1}(x, g_2) \\ D_{x_2}(x, g_2) \\ D_{x_3}(x, g_2) \end{pmatrix} \quad (9a)$$

Sprott Oscillator-2 after coupling:

$$\begin{pmatrix} \dot{y}_1 \\ \dot{y}_2 \\ \dot{y}_3 \end{pmatrix} = \begin{pmatrix} -b_2 \cdot y_2 \\ y_1 + y_3 \\ y_1 + y_2^2 - y_3 \end{pmatrix} + \begin{pmatrix} D_{y_1}(y, g_1) \\ D_{y_2}(y, g_1) \\ D_{y_3}(y, g_1) \end{pmatrix} \quad (9b)$$

The mutual interaction between the oscillators is now established in (9a) and (9b) using coupling terms  $D_{x_i}(x, g_2)$  and  $D_{y_i}(y, g_1)$ , ( $i=1, 2, 3$ ). This Sprott system is not inversion symmetric as seen from its dynamical flow.

**Case-I:** The CS or AS is realized by altering the size of oscillator-2 and keeping oscillator-1 unchanged. For identical systems,  $b_1=b_2=b$ , the *Jacobian* of the interacting systems are,

$$J_1 = \begin{bmatrix} 0 & -b & 0 \\ 1 & 0 & 1 \\ 1 & 2y_2 & -1 \end{bmatrix} \quad J_2 = \begin{bmatrix} 0 & -b & 0 \\ 1 & 0 & 1 \\ 1 & 2\alpha x_2 & -1 \end{bmatrix} \quad (10)$$

The  $H$  matrix is constructed from the *Jacobian* by replacing its element connected to the state variable by a constant  $p$ ,

$$H = \begin{bmatrix} 0 & -b & 0 \\ 1 & 0 & 1 \\ 1 & p & -1 \end{bmatrix} \quad (11)$$

The characteristic equation 7(a) of the  $H$  matrix in (11) is easily obtained where its parameters are defined as  $a_1=1, a_2=b-p, a_3=2b$ . It can be checked that the RH criterion (7b) is satisfied

for a choice of  $p < -b$ . This makes the  $H$  matrix to be a Hurwitz with its eigenvalues all having negative real parts, and thereby the asymptotically stable synchronization between the mutually coupled oscillators is established. By substituting (10) and (11) in 3(c)-(d) and assuming  $S_x=S_y=0.5$ , the coupling terms are,

$$\begin{pmatrix} D_{x_1}(x, g_2) \\ D_{x_2}(x, g_2) \\ D_{x_3}(x, g_2) \end{pmatrix} = \begin{pmatrix} 0 \\ 0 \\ 0.5(p-2y_2)(x_2 - \frac{y_2}{\alpha}) \end{pmatrix} \quad (12)$$

$$\begin{pmatrix} D_{y_1}(y, g_1) \\ D_{y_2}(y, g_1) \\ D_{y_3}(y, g_1) \end{pmatrix} = \begin{pmatrix} 0 \\ 0 \\ \alpha(1-\alpha)x_2^2 + 0.5(p-2\alpha x_2)(y_2 - \alpha x_2) \end{pmatrix}$$

In (12),  $p=-1$  and  $\alpha=-2$  are chosen to realize AS and amplification in oscillator-2. Numerical results of two mutually coupled Sprott oscillators (9a) and (9b) with coupling term (12) are presented in Fig.1. The 2D projection of both the oscillators are shown in Fig.1(a): oscillator-1 is plotted as  $x_1$  vs  $x_3$  in solid line and oscillator-2 is plotted as  $y_1$  vs  $y_3$  in dotted line. The oscillator-1 is in original size and the oscillator-2 is inverted and amplified as expected for  $\alpha=-2$ . The  $x_1$  vs.  $y_1$  plot in Fig.1(b) confirms AS between the oscillators. The time series plots in Fig.1(c)-(e) show that all three similar pairs of state variables are in AS state while  $x_i$  in solid lines for oscillator-1 is smaller than  $y_i$  in dotted lines for oscillator-2. All three error functions,  $e_i=(y_i+2x_i)$ ,  $i=1,2,3$  in Fig.1(f) show that they exponentially converges to zero and it confirms that oscillator-2 is inverted and amplified by a factor of two.

**Case-II:** The CS or AS is realized by altering the size of oscillator-1 and keeping oscillator-2 unchanged. The coupling terms are now defined using (8a) and (8b),

$$\begin{pmatrix} D_{x_1}(x, g_2) \\ D_{x_2}(x, g_2) \\ D_{x_3}(x, g_2) \end{pmatrix} = \begin{pmatrix} 0 \\ 0 \\ \alpha(1-\alpha)y_2^2 + 0.5(p-2\alpha y_2)(x_2 - \alpha y_2) \end{pmatrix} \quad (13)$$

$$\begin{pmatrix} D_{y_1}(y, g_1) \\ D_{y_2}(y, g_1) \\ D_{y_3}(y, g_1) \end{pmatrix} = \begin{pmatrix} 0 \\ 0 \\ 0.5(p-2x_2)(y_2 - \frac{x_2}{\alpha}) \end{pmatrix}$$

To realize CS and amplification in the oscillator-1,  $p=-1$  and  $\alpha=2$  are chosen. Numerical results are presented in Fig.2. The 2D projection of both the oscillators are shown in Fig.2(a): oscillator-1 is plotted as  $x_1$  vs.  $x_3$  shown in dotted line and oscillator-2 is plotted as  $y_1$  vs  $y_3$  shown in solid line. It is clearly seen that oscillator-1 is amplified in size than the oscillator-2, as expected for  $\alpha=2$ . The  $y_1$  vs.  $x_1$  plot in Fig.1(b) confirms CS between the oscillators. Alternatively, a CS state can be realized in Case I while AS can be realized in Case II. It is only a matter choice of the sign of  $\alpha$ .

#### IV. OPCL COUPLING: EXPERIMENT

An electronic circuit of the Sprott oscillators and the coupling are designed and, the method of targeting and control of synchronization is implemented. As discussed in the previous section, the choice of the sign of  $\alpha$  decides the type of synchronization and their magnitude decides the scale of the attractor size. It is shown that this parameter is accessible and can be precisely tuned to control synchronization and to induce a smooth transition from one to the other form of synchronization without loss of synchrony.

##### A. Bidirectional Mode

The circuit of two mutually coupled Sprott oscillators (9a) and (9b) and the coupling (12) is shown in Fig.3. The oscillator-1 (OS1) is constructed using three inverting integrators (U1, U3-U4:  $\mu$ A741), one inverting amplifier (U2:  $\mu$ A741) and one multiplier (UA1:AD633). The integrators derive three corresponding state variables as their dynamic output voltages while the multiplier derives the only single quadratic nonlinearity in the Sprott system 9(a). The oscillator-2 (OS2) is constructed, in a similar fashion, using three integrators (U5, U7-U8), one inverter U6 ( $\mu$ A741) and one multiplier UA2 (AD633).  $R_1$  or  $R_9$  decides the  $b$  parameter. Taking  $\alpha=-2$  and  $p=-1$ , the coupling circuit is built using three multipliers (UA3-UA5) and two summing amplifier (U9,U12) and two inverting amplifiers (U10-U11). The output voltages of (U1,U3,U4) of OS1 oscillator and (U5,U7,U8) of OS2 oscillator are the analogs of  $(x_1, x_2, x_3)$  and  $(y_1, y_2, y_3)$  respectively. Four variables at a time (two similar pairs of voltages from two oscillators) are measured using a 4-channel digital oscilloscope (Yokogawa DL9140, 1GHZ, 5GS/s). Experimental observations are shown in Fig.4. *Upper row:* 2D projection of the OS1 attractor is shown at left as a plot of outputs of U1 ( $x_1$ ) vs. U4 (actually observed inverted  $x_3$ ). The 2D projection of the OS2 attractor is plotted in the middle using outputs of U5 ( $y_1$ ) vs. U8 (inverted  $y_3$ ). All axes are in same scale to confirm that OS2 is inverted and enlarged while OS1 remains unchanged. The OS2 attractor is actually enlarged twice compared to the OS1 attractor. The plot of outputs of U1 ( $x_1$ ) vs. U5 ( $y_1$ ) at right confirms AS. *Lower row:* Time series measured at outputs of U1 ( $x_1$ ) and U5 ( $y_1$ ) is shown at left, outputs of U3 ( $x_2$ ) and U7 ( $y_2$ ) in the middle and, U4 ( $x_3$ ) and U8 ( $y_3$ ) at right and confirms that OS1 and OS2 are in AS. Lower time series of OS2 in all three panels are clearly enlarged twice and in AS with upper time series of OS1. Experimental results in Fig.4 are clearly in good agreements with numerical results in Fig.1. By appropriate choice of  $\alpha$ , one can also realize CS with amplification or attenuation.

##### B. Unidirectional Mode

For unidirectional mode the OPCL coupling is easily obtained by taking  $S_x=0$ ,  $S_y=1$  in 3(c)-(d). Obviously, the coupling term is present in one of the oscillators only. To implement the coupling in experiment, the Sprott models in (9a) and (9b) are used again when the coupling term is defined by,

$$D_{y_3}(y, g_1) = \alpha(1 - \alpha)x_2^2 + (p - 2\alpha x_2)(y_2 - \alpha x_2) \quad (14)$$

All other coupling terms in (9a) and (9b) are zero. The driver in (9a) and the response in (9b) are chaotic before coupling for  $b_1 = b_2 = 0.22$ . With a choice of  $p = -1$ , one can realize CS ( $\alpha = 1$ ), AS ( $\alpha = -1$ ), amplification ( $\alpha > \pm 1$ ), attenuation ( $\alpha < \pm 1$ ) and amplitude death ( $\alpha = 0$ ). The circuit of the coupled Sprott system is shown in the Fig.5. The Sprott oscillators are designed in a similar way as shown in Fig.3. The driver circuit is constructed using three inverting integrators with output at each node labeled by  $V_{x1}$ ,  $V_{x2}$ ,  $V_{x3}$  and an inverting amplifier used to invert the  $V_{x1}$  signal and, a multiplier IC AD633 (UA1). Similarly the response circuit is constructed with nodes labeled as  $V_{y1}$ ,  $V_{y2}$ ,  $V_{y3}$ . Using Kirchoff's laws at the nodes, the dynamical equations of the coupled Sprott oscillators are derived:

*Driver:*

$$\begin{aligned} RC \frac{d(V_{x1})}{dt} &= -\frac{R}{R_1} V_{x2} \\ RC \frac{d(V_{x2})}{dt} &= V_{x1} + V_{x3} \\ RC \frac{d(-V_{x3})}{dt} &= V_{x1} + \frac{R}{R_2} \frac{V_{x2}^2}{10} - V_{x3} \end{aligned} \quad (15)$$

*Response:*

$$\begin{aligned} RC \frac{d(V_{y1})}{dt} &= -\frac{R}{R_3} V_{y2} \\ RC \frac{d(V_{y2})}{dt} &= V_{y1} + V_{y3} \\ RC \frac{d(-V_{y3})}{dt} &= V_{y1} + \frac{R}{R_4} \frac{V_{y2}^2}{10} - V_{y3} + D(V_y, \alpha V_x) \end{aligned} \quad (16)$$

The coupling circuit  $D(y, \alpha x)$  is obtained from (14) with a choice of  $p = -1$ , and expressed in terms of circuit components

$$D(V_y, \alpha V_x) = -V_{y2} + \alpha V_{x2} + \frac{R}{R_{10}} \frac{\alpha V_{x2}^2}{10} \left( \alpha V_{x2} + V_{x2} - \frac{R}{R_8} V_{y2} \right) \quad (17)$$

where  $\alpha$  is analogous to a constant voltage measured at node  $V_c$ . The  $V_c$  is obtained using a voltage divider network with  $\pm 12$ VDC and resistances  $R_5$ ,  $R_6$  and a slow variable potentiometer,  $R_7$  (20k $\Omega$ ). Voltage drops at nodes  $V_a$  and  $V_b$  are +2.4V and -2.4V for the choice of  $R_5 = R_6 = 40$ k $\Omega$ . The provision of upper ( $V_a$ ) and lower voltage cutoffs ( $V_b$ ) is made to secure the value of scaling factor  $\alpha$  within the specific range ( $\alpha = \pm 2.4$ ). By slowly varying the potentiometer  $R_7$ , a continuous and smooth change from +2.4V to -2.4V is induced at node  $V_c$ . Effectively  $\alpha$  is thereby varied from +2.4 to -2.4. One can now easily control synchronization by making a smooth transition from CS to AS between OS1 and OS2, where the polarity of voltage at node  $V_c$  decides the type of synchrony and a change in voltage level at  $V_c$  alters the size of the response attractor. At the intermediate value,  $V_c = 0$  ( $\alpha = 0$ ), the response oscillator is forced to oscillation death. All throughout this transition process, the response oscillator never loses synchrony with the driver. A precise and smooth control of synchronization and scaling of the response attractor size is thereby implemented.

The oscilloscope pictures(Yokogawa DL9140, 1GHZ, 5GS/s) are presented in Fig.6. *Upper row:* An array of 2D projections of oscillator-2 (OS2) is plotted  $V_{y1}$  vs.  $V_{y2}$  from left to right as measured for different  $\alpha$  values. OS2 attractor size is larger at left, second from left is identical to the original size and reduced to zero size in the middle. Then it become identical to original size at right to the middle and, amplified at right but in opposite phase. This variation in size is stimulated by the  $V_c$  or its analog  $\alpha$  parameter. Left panel shows OS2 is amplified 2.4 times to OS1 for a choice of  $\alpha=2.4$ , second from the left shows OS2 identical in size to OS1 for  $\alpha=1$ , amplitude death of OS2 for  $\alpha=0$  at center, second from the right shows OS2 is again identical to OS1 for  $\alpha=-1$  but opposite facing, right side shows OS2 is 2.4 times larger to OS1 and opposite facing for  $\alpha=-2.4$ . *Middle row:* An array of 2D projections plotted  $V_{y1}$  vs  $V_{x1}$ , where  $V_{y1}$  in the  $x$ -axis and  $V_{x1}$  in the  $y$ -axis manifesting the synchronization manifold. All axes are in the same scale. Each of these oscilloscope pictures corresponds to the picture exactly in the upper row. First two plots of the left confirm that OS1 and OS2 are CS for positive values of  $\alpha=(2.4, 1)$ , center shows amplitude death of OS2 for  $\alpha=0$ , and last two plots at the right confirm that OS1 and OS2 are in AS for negative values of  $\alpha=(-2.4, -1)$ . *Lower row:* Time series of OS1 and OS2 measured at  $V_{x1}$  and  $V_{y1}$  are plotted for three different  $\alpha$  values. At left, OS2 is amplified compared to OS1 in CS mode( $\alpha=2.4$ ), at center, OS2 is in amplitude death while OS1 is oscillatory, at right OS2 is amplified compared to OS1 but in AS mode( $\alpha=-2.4$ ).

## V. CONCLUSION

An open-plus-closed-loop (OPCL) coupling design is explored for engineering synchronization in chaotic oscillators. A general scheme is described as applicable for unidirectional as well as bidirectional coupling mode, which is capable to realize a desired response such as CS, AS states in chaotic systems. A scaling factor is introduced in the definition of coupling that allows amplification or attenuation of one attractor relative to another. The theoretical details of the method how to design the OPCL based coupling is given and illustrated with numerical examples of a Sprott system. The OPCL based coupling design is physically implemented for unidirectional and bidirectional modes in electronic circuits using Sprott oscillators. It is demonstrated through an experiment that by continuously varying a scaling factor one can make a transition from CS to AS via AD in a response oscillator under unidirectional coupling mode. A precise and smooth control of synchronization in chaotic oscillators is implemented in electronic circuit. Most importantly, contrary to conventional techniques, the coupled system never loses stability during a transition from one to the other form of synchronization.

## REFERENCES

- [1] A. S. Pikovsky, M. G. Rosenblum, and J. Kurths, "Synchronization: A Universal Concept in Nonlinear Science", Cambridge University Press, Cambridge, 2001.
- [2] S. Strogatz, "Sync: How order emerges from chaos in the Universe, Nature and Daily Life", Hyperion, New York, 2003.
- [3] L. M. Pecora and T. L. Carroll, "Synchronization in chaotic systems", *Phys. Rev. Lett.*, vol. 64, no.8, pp.821-824, 1990.
- [4] T. Yamada, H. Fujisaka, "Stability Theory of Synchronized Motion in Coupled-Oscillator Systems. III", *Prog. Theor. Phys.*, vol.72, no. 5, pp.885-894, 1984.
- [5] A. Argyris, D. Syvridis, L. Larger, V. Annovazzi-Lodi, P. Colet, I. Fischer, J. Garcia-Ojalvo, C. R. Mirasso, L. Pesquera and K. Alan Shore, "Chaos-based communications at high bit rates using commercial fibre-optic links" *Nature*, vol. 438, pp. 343-346, 2005.
- [6] D.J. Gauthier and J.C. Bienfang, "Intermittent loss of synchronization in coupled chaotic oscillators: toward a new criterion for high-quality synchronization", *Phys. Rev. Lett.*, vol. 77, no.9, pp 1751-1755, 1996.
- [7] S.C. Venkataramani, B.R. Hunt, E. Ott, D.J. Gauthier, and J.C. Bienfang, "Transitions to Bubbling of Chaotic Systems", *Phys. Rev. Lett.*, vol. 77, no.27, pp. 5361-5364, 1996.
- [8] L. M. Pecora and T. L. Carroll, "Master Stability Functions for Synchronized Coupled Systems," *Phys. Rev. Lett.*, vol. 80, no.10, pp. 2109-2112, 1998.
- [9] Y. Chen, G. Rangarajan, and M. Ding, "General stability analysis of synchronized dynamics in coupled systems", *Phys. Rev. E*, vol. 67, no. 2, 026209, 2003.
- [10] S. Taherion, Y.-C.Lai, "Observability of lag synchronization of coupled chaotic oscillators", *Phys. Rev. E*, vol. 59, no.6, pp. R6247-R6250, 1999.
- [11] M. G. Rosenblum, A. S. Pikovsky, and J. Kurths, "From Phase to Lag Synchronization in Coupled Chaotic Oscillators", *Phys. Rev. Lett.*, vol. 78, no.22, pp. 4193-4196, 1997.
- [12] M. G. Rosenblum, A.S. Pikovsky, J. Kurths, "Phase Synchronization of Chaotic Oscillators", *Phys. Rev. Lett.*, vol. 76, no.11, pp. 1804-1807, 1996.
- [13] S. K. Dana, B. Blasius, J. Kurths, "Experimental evidence of anomalous phase synchronization in two diffusively coupled Chua oscillators", *Chaos*, vol. 16, no. 2, 023111, 2006.
- [14] D. He and L. Stone, "Spatio-temporal synchronization of recurrent epidemics", *Proc. R. Soc. London*, vol. 270, no.1523, pp. 1519-1526, 2003.
- [15] N. F. Rulkov, M.M. Sushchik, L.S. Tsimring, H.D.I. Abarbanel, "Generalized synchronization of chaos in directionally coupled chaotic systems", *Phys. Rev. E*, vol. 51, no.2, pp. 980-994, 1995.
- [16] D. Terman, N. Kopell and A. Bose, "Dynamics of two mutually coupled slow inhibitory neurons", *Physica D: Nonlinear Phenomena*, vol. 117, no. 1-4, pp 241-275, 1998.
- [17] E. M. Izhikevich, "Dynamical Systems in Neuroscience: The Geometry of Excitability and Bursting", MIT Press, Cambridge, 2007.
- [18] L. S. Tsimring, N. F. Rulkov, M. L. Larsen and M. Gabbay, "Repulsive Synchronization in an Array of Phase Oscillators" *Phys. Rev. Lett.*, 95, no.1, 014101, 2005.
- [19] C.G. Rusin, H. Kori, I.Z. Kiss, J. L. Hudson, "Synchronization engineering: tuning the phase relationship between dissimilar oscillators using nonlinear feedback" *Phil. Trans. R. Soc. A*, vol. 368, pp 2189-2204, 2010.
- [20] O. V. Popovych, P.A. Tass, "Synchronization control of interacting oscillatory ensembles by mixed nonlinear delayed feedback", *Phys. Rev. E*, vol. 82, no. 2, 026204, 2010.
- [21] K. Pyragas, T. Pyragienė, "Coupling design for a long-term anticipating synchronization of chaos" *Phys. Rev. E*, vol. 78, no. 4, 046217, 2008.
- [22] I. Grosu, "Robust synchronization", *Phys. Rev. E*, vol. 56, no.3, pp. 3709-3712, 1997.
- [23] I. Grosu, E. Padmanaban, P. K. Roy, S. K. Dana, "Designing Coupling for Synchronization and Amplification of Chaos" *Phys. Rev. Lett.*, vol. 100, 234102, 2008.
- [24] I. Grosu, R. Banerjee, P. K. Roy, S. K. Dana, "Design of coupling for synchronization of chaotic oscillators", *Phys. Rev. E*, vol. 80, no.1, 016212, 2009.
- [25] J. C. Sprott, "Some simple chaotic flows", *Phys. Rev. E*, vol. 50, no.2, pp. R647-R650, 1994.

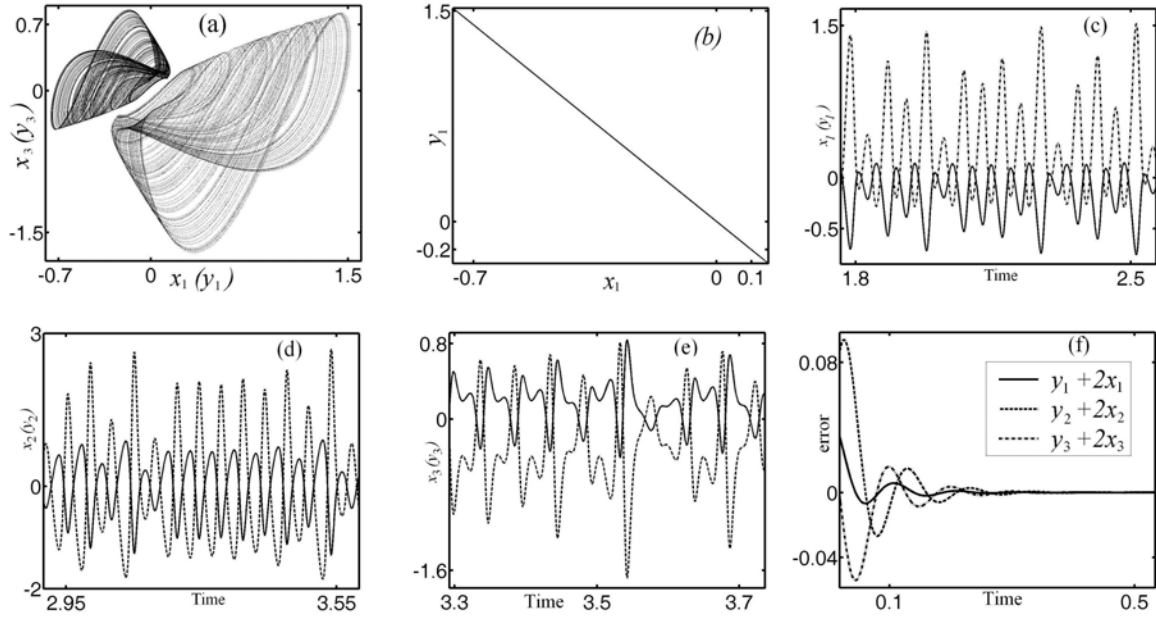


Fig.1. Coupled Sprott oscillators [ $b_1=b_2=0.25, p = -1, \alpha = -2$ ]: (a) 2D attractor of oscillator-1 and oscillator-2 (amplified and inverted), (b) plot of  $x_1$  vs.  $y_1$  in AS state. Time series of  $(x_1, y_1)$  in (c),  $(x_2, y_2)$  in (d) and  $(x_3, y_3)$  in (e). Plot of errors,  $e_i = (y_i + 2x_i)$  in (f).

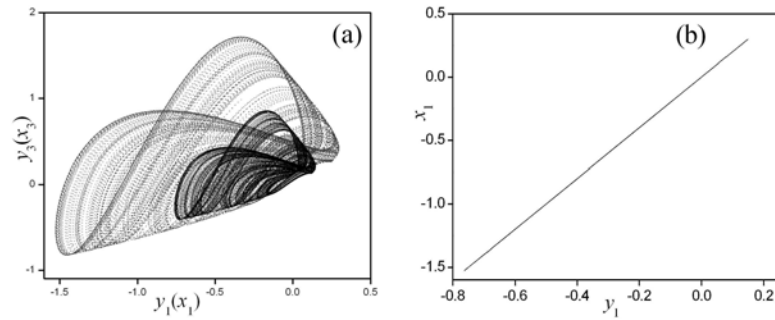


Fig.2. Coupled Sprott oscillators [ $b_1=b_2=0.25, p = -1, \alpha = 2$ ]: (a) 2D attractor of oscillator-1 (amplified version in dotted line) and oscillator-2 (solid line), (b) plot of  $y_1$  vs.  $x_1$  in CS state.

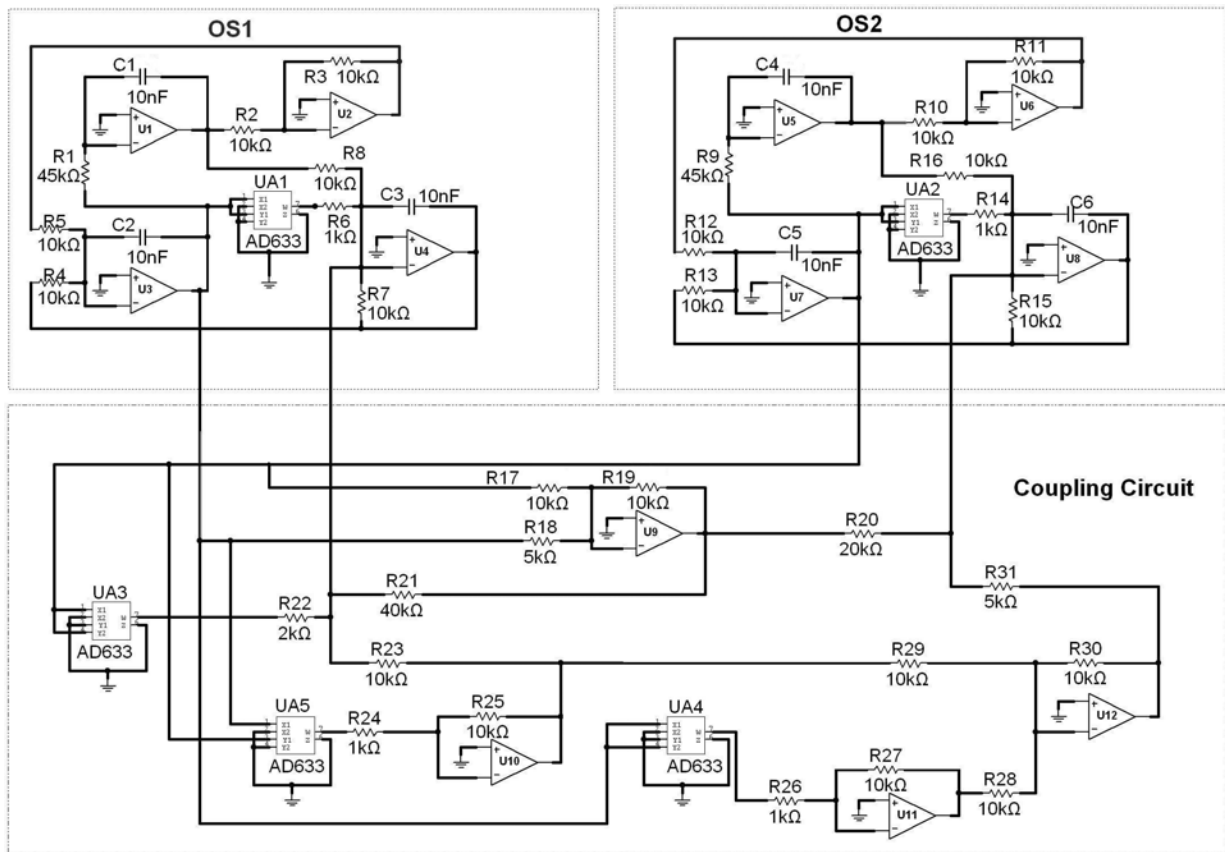


Fig.3. Two mutually coupled Sprott circuits: inverting integrators U1-U4 (U5-U8), multipliers AD633 UA1 (UA2), resistances R1-R8 (R9-16) and capacitances C1-C3 (C4-C6) are used to design the OS1 and OS2. The coupling circuit is composed of summing amplifiers (U9-U12), multipliers (UA3-UA5) with resistances R17-R31. Components values (1% tolerance) are noted in the circuit.

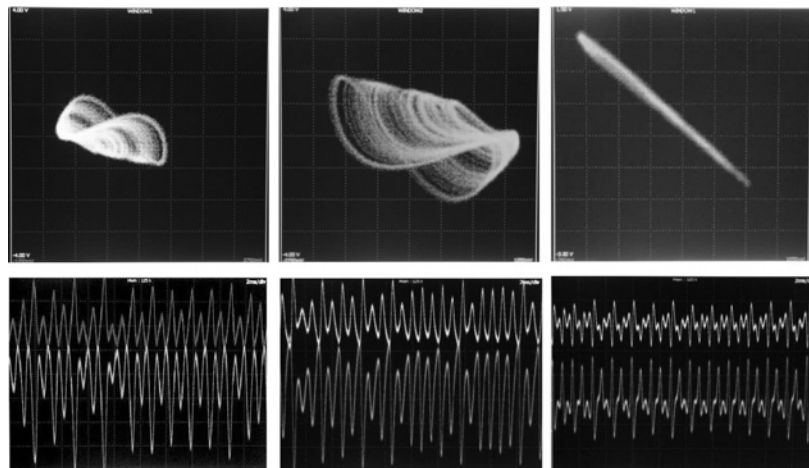


Fig.4. Oscilloscope pictures. Upper row: 2D attractor of oscillator-1 at left, its amplified and inverted version in the middle of oscillator-2; axes in same scale. Output voltages of U1 (500mV/div.) vs. U5 (1V/div.) at right confirm AS. Lower row: time series measured at U1 (upper) and U5 (below) at left, U3 (upper) and U7 (below) at middle and U4 (upper) and U8 (below) at right confirm AS and amplification.

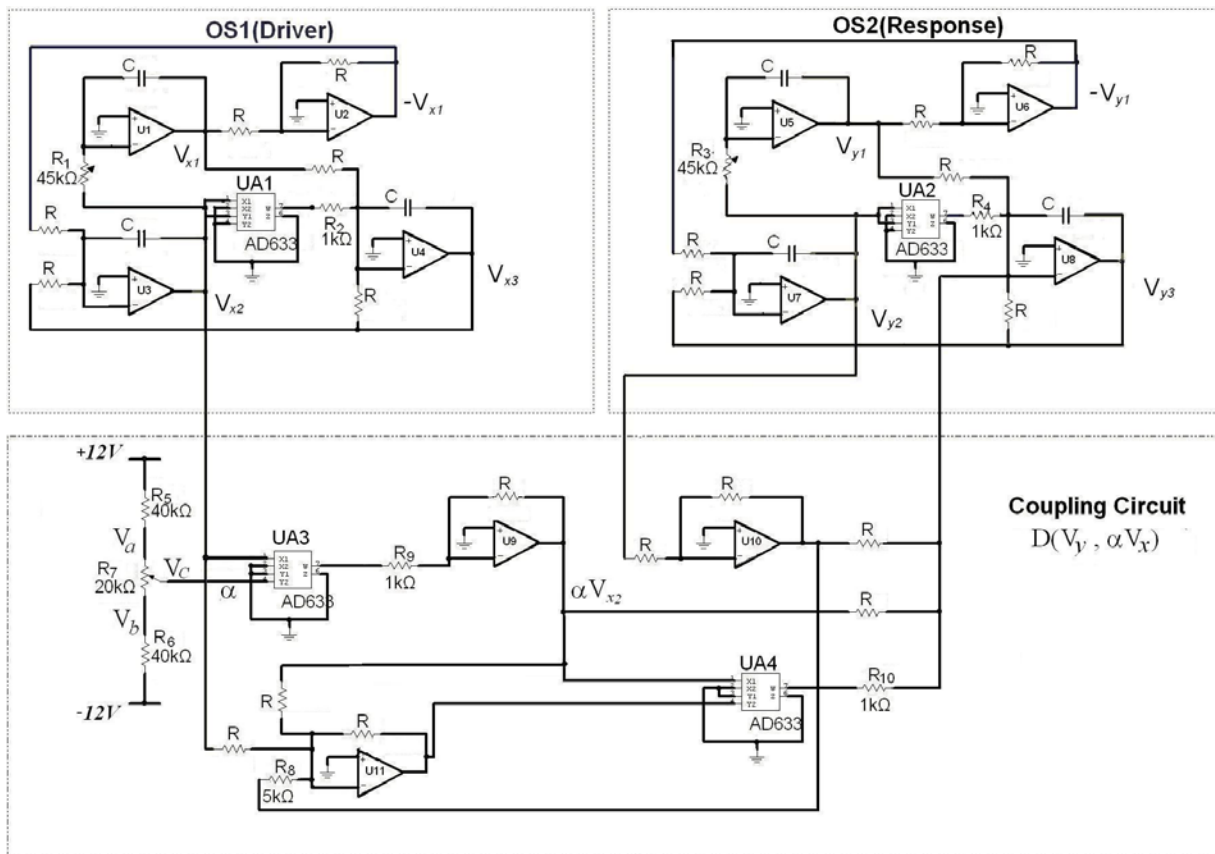


Fig.5 Coupled Sprott circuit: Inverting integrators U1-U4 (U5-U8), multipliers AD633 UA1(UA2), resistances R(10 kΩ) and capacitances C(10 nF) and labeled resistances with value are used to design the OS1 and OS2. The coupling circuit is composed of summing amplifiers, multipliers with resistances. Components values (1% tolerance) are noted in the circuit.

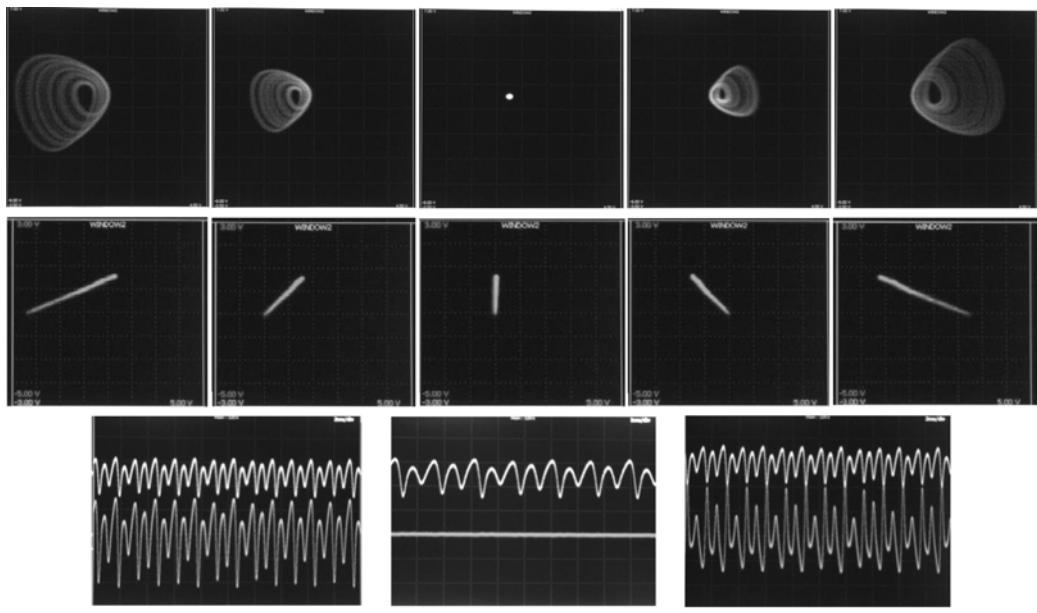


Fig.6. Oscilloscope pictures. Upper row: An array of 2D attractors of response from left to right side of different mode of synchronization, CS with amplification, CS, AD, AS, AS with amplification. Middle row: Output voltages of U1 vs. U5 plotted at different  $\alpha$  value (2.4,1,0,-1,-2.4). Lower row: time series measured at U1 (upper) and U5 (below) at different  $\alpha$  value: at left  $\alpha = 2.4$ (CS), at middle  $\alpha = 0$ (AD) and at right  $\alpha = -2.4$ (AS).